Role of TNF-α and the NF-κB pathway in drug-induced organ injuries

Benedetti, G.O.E.

4

TNF–α–mediated NF–κB survival signalling impairement by cisplatin enhances JNK activation allowing synergistic apoptosis of renal proximal tubular cells

Giulia Benedetti, Lisa Fredriksson, Bram Herpers, John Meerman, Bob van de Water and Marjo de Graauw

Division of Toxicology, Leiden/Amsterdam Center for Drug Research, Leiden University, The Netherlands

Biochem Pharmacol. 2013 Jan 15;85(2):274-86

Abstract

Cisplatin-induced nephrotoxicity is an important limiting factor for cisplatin use. Tumor necrosis factor α (TNF-α) is known to contribute to cisplatin-induced nephrotoxicity by inducing an inflammatory process aggravating the primary injury, thereby resulting in acute kidney injury (AKI). The present study investigates the pathways synergistically activated by cisplatin and TNF-α responsible for TNF-α-enhanced cisplatin-induced renal cell injury. To do so, immortalized renal proximal tubular epithelial cells (IM-PTECs) were co-treated with TNF-α and cisplatin. Under these conditions, cisplatin induced dose-dependent apoptosis in IM-PTECs, which was significantly enhanced by TNF-α. Transcriptomic analysis revealed that cisplatin inhibited the typical TNF-α response and cisplatin/TNF-α treatment up-regulated cell death pathways while it down-regulated survival pathways compared to cisplatin alone. In concordance, the gene expression levels of kidney injury markers combined with activation of specific inflammatory mediators were enhanced by cisplatin/TNF-α treatment, resembling the *in vivo* cisplatin-induced nephrotoxicity response. Furthermore, combined cisplatin/TNF-α treatment inhibited NF-κB nuclear translocation and NF-κB-mediated gene transcription leading to enhanced and prolonged JNK and c-Jun phosphorylation. JNK sustained activation further inhibited NF-κB signalling via a feedback loop mechanism. This led to an alteration in the transcription of the NF-κB-induced anti-apoptotic genes c-IAP2, Bcl-XL, Bruce and Bcl2 and pro-apoptotic genes Bfk and Xaf1 and consequently to sensitization of the IM-PTECs towards cisplatin/TNF-α-induced toxicity. In conclusion, our findings support a model whereby renal cells exposed to both cisplatin and TNF-α switch into a more pro-apoptotic and inflammatory program by altering their NF-κB/JNK/c-Jun balance.

1. Introduction

Cisplatin is a chemotherapeutic agent widely used for the treatment of several types of cancers (1). However, its use is mainly limited by nephrotoxicity. More than one-third of the patients develop renal injury within 10 days after a single dose of cisplatin (2). Cisplatin nephrotoxicity is a complex multi-factorial process affecting mainly the proximal tubular epithelial cells (PTECs). Cisplatin is actively transported into these cells, followed by activation of several stress signalling cascades such as oxidative stress pathways, mitogen-activated protein kinase-signalling pathways (MAPKs), p53 signalling pathway and both extrinsic and intrinsic apoptosis pathways (3). Activation of these pathways leads to renal cell injury. Furthermore, in the kidney an

inflammatory response is initiated, which exacerbates the primary renal injury caused by cisplatin leading to acute kidney injury (AKI) (3, 4). This inflammation is initiated via the production of the cytokine tumor necrosis factor-α (TNF-α), by the resident kidney cells (5) including the proximal tubular cells themselves (6, 7) and simultaneously or secondarily by infiltrating immune cells (8).

TNF-α is known to promote cell survival or cell death by tightly regulated mechanisms. Binding to the TNF receptors TNFR1 and TNFR2 leads to recruitment of one of two complexes. Complex I activates the transcription factor nuclear factor κB (NF-κB), leading to transcription of inflammatory and survival genes (9). Complex II, which is assembled only when TNFR1-associated death domain protein (TRADD) and receptor-interacting protein 1 (RIP1) are ubiquitinated, activates caspase-8 and -10 leading to the induction of apoptosis (10). In addition, TNF-α activates MAPKs including c-Jun N-terminal kinases (JNKs) (11). The state of JNK activation eventually determines cellular outcome. While transient JNK activation is associated with cell survival, prolonged activation results in cell death (12). Under normal conditions, activation of the caspase-8 complex and prolonged JNK activation are antagonized by different NF-κB pro-survival target genes. We have previously shown that co-exposure of hepatocytes to the hepatotoxicant diclofenac and TNF-α deregulated NF-κB activity and prolonged JNK activation as well as increased caspase-8 complex formation (13). These perturbations led to an enhancement of hepatocyte cell death. In the kidney, TNF-α contributes to cisplatin nephrotoxicity by inducing both inflammation and renal cell death. Inhibition of TNF-α via pharmacological inhibitors or antibodies ameliorated cisplatin-induced nephrotoxicity *in vivo* (14). However, it is not yet clear which pathways, synergistically (de)activated by cisplatin and TNF-α, lead to renal injury.

In this study, immortalized proximal tubular epithelial cells (IM-PTECs) were used to investigate the cisplatin/TNF-α interaction. Cisplatin induced a dose-dependent cell death of IM-PTECs, which was enhanced by the cytokine TNF-α. Transcriptomic analysis revealed that cisplatin inhibited the typical TNF-α response and combined cisplatin/TNF-α treatment increased cell death pathways compared to cisplatin alone. The increased cell death observed with the combined cisplatin/TNF-α treatment enhanced the gene expression levels of kidney injury markers and of specific inflammatory genes mimicking the cisplatin-induced nephrotoxicity response observed *in vivo*. Furthermore, with the combined cisplatin/TNF-α treatment, inhibition of the NF-κB signalling led to an enhancement of JNK and c-Jun phosphorylation. JNK sustained activation led to further inhibition of the NF-κB signalling via a feedback loop mechanism. The transcription of NF-κB-induced anti-apoptotic genes was reduced accompanied by

an enhancement of the transcription of pro-apoptotic genes sensitizing the IM-PTECs towards cisplatin/TNF-α treatment. Our findings support a model whereby the renal cells exposed to both cisplatin and TNF-α switch into a more pro-apoptotic and inflammatory program by altering their NF-κB/JNK/c-Jun balance.

2. Material and methods

2.1. Reagents and antibodies

Mouse recombinant TNF-α was acquired from R&D Systems (Abingdon, UK). The selective IKKα/β inhibitor wedelolactone, cis-diamminedichloroplatinum(II) (cisplatin), doxorubicine, etoposide, methyl methanesulfonate (MMS) and tunicamycin were from Sigma-Aldrich (Zwijndrecht, The Netherlands). The selective JNK inhibitor SP600125 was from Enzo Life Sciences (Zandhoven, Belgium). The irreversible pan-caspase inhibitor z-VAD-fmk was from Bachem (Weil am Rhein, Germany). AnnexinV-Alexa488 was made as described (15). The antibody against tubulin was from Sigma-Aldrich, the antibody against NF-κB (p65) was from Santa Cruz (Tebu-Bio, Heerhugowaard, The Netherlands) and the phospho-specific JNK antibody (Thr183/Tyr185) was from New England Biolabs (Leusden, The Netherlands). The antibodies against phospho-specific c-Jun (Ser63), phospho-specific IκBα (Ser32), IκBα and JNK1/2 were from Cell Signalling (Bioké, Leiden, The Netherlands).

2.2. Cell culture

Immortalized proximal tubular cells (IMPTECs) described previously (16) were cultured at 33°C in HK2 medium (DMEM/F12 medium (Invitrogen, Breda, The Netherlands) with 10% fetal bovine serum (Hyclone, Etten-Leur, The Netherlands), 5 µg/ml insulin and transferrin, 5 ng/ml sodium selenite (Roche, Almere, The Netherlands), 20 ng/ml triiodo-thyrionine (Sigma-Aldrich), 50 ng/ml hydrocortisone (Sigma-Aldrich), and 5 ng/ml prostaglandin E1 (Sigma- Aldrich) with L-glutamine and antibiotics (both from Invitrogen) and mouse interferon-γ (IFN-γ) (1 ng/ml; R&D Systems, Abingdon, England)) in 5% CO2 and 95% air between passage 3 and 20. Prior to each experiment, the cells were differentiated into proximal tubular cells by culturing them for 4 days in restrictive conditions (at 37°C in the absence of IFN-γ). The cells were then plated in the appropriate assay plates and cultured for 2 more days. In total, IMPTECs were cultured in restrictive conditions for 6 days, allowing the disappearance of SV40 activity and completion of differentiation (16).

2.3. Exposures

IM-PTECs were exposed to various concentrations of cisplatin or vehicle ± 8 ng/ml TNF-α. Exposure to TNF-α was performed 30 minutes prior to cisplatin. Incubation with the inhibitors SP600125 and wedelolactone was done 30 minutes prior the addition of TNF-α and followed 30 minutes later by the exposure to cisplatin.

IM-PTECs were exposed to the DNA damaging agents doxorubicine 3 μM, etoposide 5 μM and MMS 50 μg/ml, and to the ER stress agent tunicamycin 10 μg/ml for 8 hours.

2.4. Cell death assays

Cell death was determined by either flow cytometry and cell cycle analysis or live cell apoptosis. Cell cycle analysis was performed by fixating the cells in ethanol during at least 24h and by subsequent staining of the cells with 3.3μM of 4,6-diamidino-2-phenylindole (DAPI). With flow cytometry (FACSCanto II; Becton Dickinson, Erembodegem, Belgium), the amount of dead cells in sub-G0/G1 was determined.

Real time induction of apoptosis was quantified using a live cell apoptosis assay previously described (15). Briefly, binding of Annexin V-Alexa488 conjugate to phosphatidyl serine present on the membranes of apoptotic cells was followed in time by imaging the cells every hour after drug exposure with a BD Pathway 855 imager (Becton Dickinson, Erembodegem, Belgium). The total area of Annexin V-Alexa488 fluorescence per image was quantified using Image Pro (Media Cybernetics, Bethesda, MD).

2.5. Western Blot

Cells were harvested as described (17). The samples were subjected to protein separation and blotted on Immobilon-P membranes (Millipore, Amsterdam, The Netherlands). Phosphorylated proteins (P-JNK, P-c-Jun and P-IκBα) were detected using the Tropix Western-Star kit™ (Applied Biosystems) following manufacturer's protocol. For tubulin, β-actin, IκBα and JNK1/2, the membranes were blocked for 1h at room temperature in milk powder 5% (w/v) in Tris-buffered saline/Tween 20 (TBST-T). Primary antibody incubation was done overnight at 4°C followed by incubation with horseradish peroxidase-conjugated or Cy5-labeled secondary antibodies (Jackson Immunoresearch, Newmarket, UK) in TBST-T for 1 h at room temperature. Protein signals were detected with ECL (GE Healthcare) followed by film detection for JNK1/2

or by visualization on the Typhoon 9400 imager (GE Healthcare, Diegem, Belgium). Ratios of protein band intensity were obtained using ImageJ 1.44i software.

2.6. Immunofluorescence

Cultured cells were stained for NF-κB p65 followed by goat anti-mouse Alexa488-labeled secondary antibody (Molecular Probes, Breda, Netherlands) and Hoechst 33258 (2 μg/ml) was used to visualize the nuclei. Cells were imaged using a Nikon TiE2000 confocal microscope (Nikon, Amstelveen, Netherlands). p65 translocation was quantified using ImagePro. Briefly, after splitting the two channels (Alexa488-stained p65 and Hoechst-stained nuclei), segmentation of individual nuclei and definition of the overall cellular area is then performed. The average intensity of p65 staining inside the nuclei is then derived.

2.7. Luciferase reporter assay

To determine the effect of cisplatin exposure and RelA inhibition/knockdown on TNF-α-induced NF-κB transcriptional activity, IMPTECs were transiently transfected with an NF-κB promoter-luciferase reporter plasmid (Clontech, Saint-Germain-en-Laye, France) using Effectene® reagent according to the manufacturer's procedures (Qiagen, Venlo, The Netherlands) and incubated for 16-18 hours. The Dual-Luciferase luciferase assay kit (Promega, Leiden, The Netherlands) and a microplate luminometer (Centro XS3 LB960, Berthold Technologies) were used to monitor luciferase activity.

2.8. Lentiviral knock-downs

Stable IM-PTECs with p65/RelA knock down were generated using lentiviral shRNA vectors (Sigma-Aldrich, in collaboration with Rob Hoeben, Leiden University Medical Centre, The Netherlands) and selection with puromycin (1 μg/ml). The plasmid encoding non-target control SHC002 was used as a control and the plasmid encoding mouse RelA number TRCN0000055343 (CCGGGCGAATCCAGACCAACAATAACTCGAGTTATTGTTGGTC TGGATTCGCTTTTTG) was used.

2.9. Gene array analysis

IM-PTECs were exposed to vehicle, cisplatin (5 μM), TNF-α (8 ng/ml) or cisplatin

in combination with TNF-α for 8 hours. Four replicates for each treatment and five for the controls were used. Total RNA was isolated from cells using an RNeasy® Mini Kit (Qiagen, Venlo, The Netherlands) according to the manufacturer's protocol. RNA concentration was determined by absorbance at 260 nm (Nanodrop Technologies, Montchanin, DE, USA), and the integrity of the RNA was checked using an Agilent 2100 Bioanalyzer (Agilent Technologies, Palo Alto, CA, USA). The synthesis of labeled cRNA and hybridization steps were performed by Service XS (Leiden, The Netherlands). Briefly, 100 ng of RNA was used to synthesize Biotin-labeled cRNA with the Affymetrix 3´ IVT Express Labeling Kit. The resulting labeled cRNA was quantified by absorbance at 260 nm (Nanodrop) and 6 µg was hybridized on an Affymetrix 24 all-in HT MG 430 PM Array plate following the procedures recommended by the manufacturer. After hybridization, the microarray slide was washed, dried, and scanned using the Hybridization, Wash and Stain Kit #901530 compatible with Affymetrix protocols. The Affymetrix Command Console (v3.0) and Expression Console software (v1.1) were used to analyze the performance of the washing, staining and scanning of the chips and to obtain background-substracted non normalized signal values.

Subsequently, these data were normalized with the BRB array Tools software (developed by Dr. Richard Simon and BRB-ArrayTools Development Team) using the Robust Multichip Average (RMA) method. Significantly differentially expressed genes (false discovery rate FDR<0.01) between the various experimental conditions were identified with an ANOVA test followed by calculation according to Benjamin and Hochberg (18). Only probes with expression levels of 2.0-fold change or more relative to the control were selected for further analysis.

Commonly deregulated genes between the different groups were identified by Venn diagrams. Classification of the selected genes according to their biological and toxicological functions was performed using the Ingenuity Pathway Analysis (IPA®) software (Ingenuity® Systems, Redwood, CA, USA). Transcription factor analysis of the most 1000 up- or down-regulated genes was performed using the Metacore software (GeneGo, MI, USA). Heatmap representations and hierarchical clustering (using Pearson correlation) were performed using the MultiArray Viewer software. Principal component analysis (PCA) was done with the Spotfire software (TIBCO, Somerville, MA, USA). The complete data set is currently submitted to ArrayExpress (EMBL-European Bioinformatics Institue, Hinxton, England; http://wwww.ebi.ac.uk/arrayexpress) and will be available for public download shortly. Accession number referencing this data set will be available on the GEO website (http://www.ncbi.nlm.nih.gov/geo/).

2.10. Quantitative real-time PCR

Total RNA was isolated from cells using an RNeasy® Mini Kit (Qiagen, Venlo, The Netherlands) according to the manufacturer's protocol. cDNA was synthesized using SuperScript® III reverse transcriptase (Invitrogen). Oligonucleotide primers (Eurogentec, Seraing, Belgium) are compiled in Table 1. Reactions were performed using qPCRSybrGreen mix (Applied Biosystems, Foster, CA, USA) on the 7900HT Fast Real-Time PCR System (Applied Biosystems, Foster, CA, USA) with an annealing temperature of 60 °C. Cycle threshold (Ct) values were normalized to the expression levels of the three housekeeping genes GAPDH, HRPT and β–tubulin. The relative expression of the genes in treated cells versus control cells was determined using the ΔCt method.

Table 1. RT-PCR primers.

Gene	Forward primer	Reverse primer
Xaf1	CTGTGGCTCTGCCTTTGAAGT	CGTCTCCTGTGGGAAGATCAG
Bfk (Bcl2l15)	CCCACTATCCCACGCTGCTA	TCCTCTCCTGAGCATGGTTCA
BCL-XL (Bcl2l1)	TGGAGTAAACTGGGGGTCGCATCG	AGCCACCGTCATGCCCGTCAGG
Bcl2	CTCGTCGCTACCGTCGTGACTTCG	CAGATGCCGGTTCAGGTACTCAGTC
c-IAP2 (Birc3)	TATTTGTGCAACAGGACATTAGGAGT	TCTTTCCTCCTGGAGTTTCCA
Bruce (Birc6)	ACATCCGACAAGCAACGGTTA	AGCACGGTGAAGGATTTCTGA

2.11. Statistical procedures

All data are expressed as mean ± standard error of the mean (S.E.M.). Statistical significance was determined by GraphPad Prism using an unpaired two-tailed t-test. The level of confidence is represented by P-values indicated in the figures.

3. Results

3.1. TNF-α enhances cisplatin-induced renal proximal tubular cell death

To investigate whether cisplatin induces cell death in our IM-PTECs, cells were exposed to increasing concentrations of cisplatin. Cisplatin induced a concentration-dependent increase in cell death as determined by cell cycle analysis (Fig. 1A) and live apoptosis imaging by following over time Annexin-V-alexa488 fluorescence (Fig. 1B).

This dose-response correlated with what is observed in patients since nephrotoxicity in patients is observed with a plasma concentration of cisplatin superior to 6 µg/ml, corresponding to an *in vitro* concentration of approximately 20 µM (19). Next, the effect of co-treatment of cisplatin and TNF-α on the cells was evaluated. *In vivo*, cisplatin-exposed renal cells secrete TNF-α resulting in activation of neighbouring cells. Cisplatin takes several days to be completely excreted in the urine (20), therefore these TNF-α pre-exposed neighbouring kidney cells are subsequently exposed to a combination of cisplatin and TNF-α. In order to mimic these sequential events observed *in vivo*, the IM-PTECs were pre-exposed to TNF-α for 30 minutes followed by cisplatin exposure. When the cells were exposed to the combined cisplatin/TNF-α treatment renal cell death was greatly enhanced (Fig. 1C and 1D). This enhancement was completely abrogated by treatment with the pan-caspase inhibitor z-VAD-fmk, indicating that TNF-α-enhanced cisplatin-induced cell death is a caspase-dependent apoptotic process (Fig. 1C and 1D). Furthermore, pre-treatment of the cells with cisplatin followed by TNF-α exposure, as well as co-treatment of the cells with cisplatin and TNF-α gave the same synergistic apoptosis than with pre-treatment of the cells with TNF-α (data not shown). Based on live cell imaging, the onset of apoptosis occurred later than 10h after exposure (Fig. 1D).

3.2. Cisplatin suppresses the TNF-α-induced transcriptional program

To obtain detailed insight into the pathways involved in the TNF-α-mediated enhancement of cisplatin-induced cell death, transcriptomic analysis was performed. IM-PTECs were exposed to TNF-α (8 ng/ml) and/or to cisplatin (5 µM) for 8 hours, a time point at which cell death did not yet occur (Fig. 1). In order to correlate the expression patterns to the cellular response observed, a PCA analysis was performed with all gene datasets. As shown in Fig. 2A, four distinct clusters can be discerned, corresponding to controls and the three treatment groups. The cisplatin/TNF-α treated group, in which high cellular injury was observed, was positioned away from the controls further in the same direction as the cisplatin group and along the principal component 2 in the same direction as the TNF-α group. This analysis suggested that the cisplatin/TNF-α group pointed towards more cell death and pro-inflammatory response than cisplatin alone but less pro-inflammatory response than TNF-α alone.

Gene expression changes with ≥ 2.0 fold-change for all conditions compared to control and FDR ≤ 0.01 were considered for further analysis and a total of 4182 genes

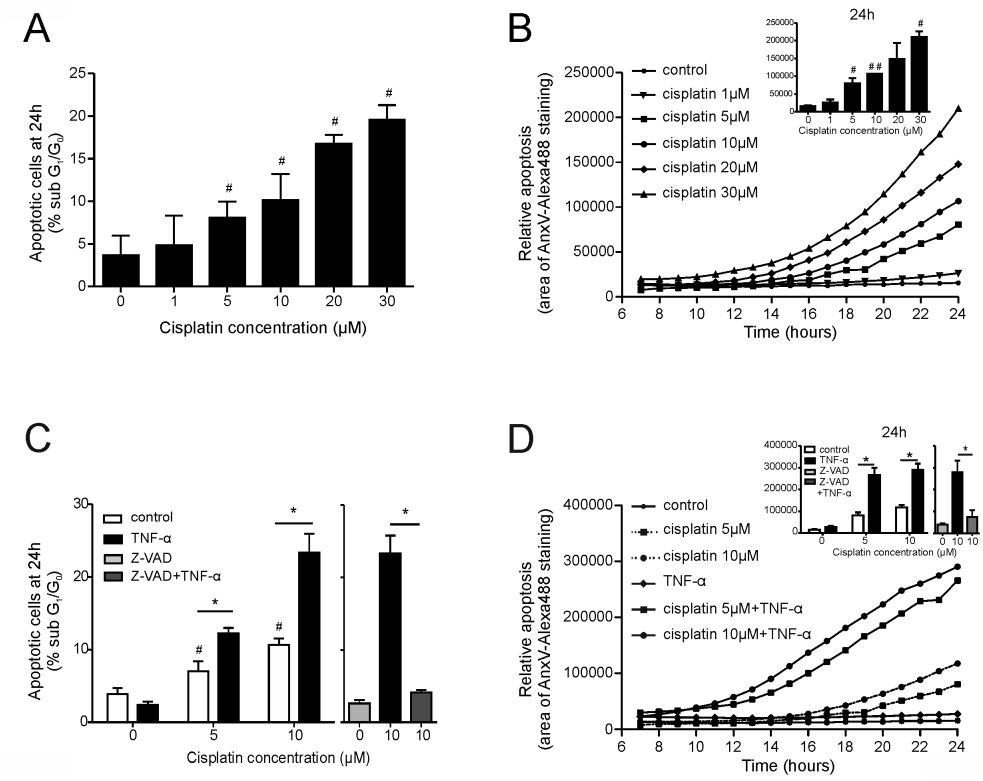

Figure 1. TNF-α enhances cisplatin-induced apoptosis in IM-PTECs. IM-PTECs were exposed to cisplatin in increasing concentrations (A and B) or were pre-exposed for 30 min with TNF-α (8 ng/ml) before cisplatin exposure (Z-VAD-fmk (100 μM) was included as indicated) (C and D). Cell death was determined by cell cycle analysis (A and C) or followed over time using Annexin V-Alexa488 staining and automated imaging on a BD pathway 855 imager (B and D). The data are represented as means of three independent experiments ± SEM. *P ≤ 0.05, **P ≤ 0.01 and #P ≤ 0.05, ##P ≤ 0.01 compared to vehicle-treated cells.

were identified with our selection criteria. Out of these genes, 3639 genes were uniquely differentially regulated with at least 2.0 fold with the combined treatment cisplatin/TNF-α. Most of these genes were differentially regulated by both cisplatin and cisplatin/TNF-α (Fig. 2B and 2C). Thereafter, these genes were divided into 1702 up-regulated genes (Fig. 2B) and 1937 down-regulated genes (Fig. 2C). The up- and down-regulated genes were then classified according to their biological and toxicological functions using Ingenuity Pathway Analysis (IPA®) software. Analysis of the up-regulated genes indicated that cisplatin/TNF-α co-treatment increased cell death compared to cisplatin or TNF-α treatment alone and that cisplatin decreased the TNF-α-induced processes (Fig. 2D). Such processes include death-receptor signalling pathways –such as TNFR1 and 2 and April-mediated signalling pathways–, cytokine signalling pathways mediated

by IL-10, IL-6 as well as immune receptors-induced signalling pathways mediated by CD27, CD40 (Fig. 2E). Analysis of the down-regulated genes revealed that basic survival processes were more affected by cisplatin/TNF-α co-treatment compared to cisplatin or TNF-α treatment alone (Fig. 2F). These processes include PTEN, mTOR, glucocorticoid receptor signalling pathways, as well as growth factor signalling (HGF, VEGF) and cAMP signalling components (PI3K, PKA) (Fig. 2G). Analysis of both up and down-regulated genes combined, as well as analysis with GeneGo Metacore™ pathway analysis software, pointed also to the same signalling pathways (data not shown). Together these data indicate that IM-PTECs treated with both cisplatin and TNF-α induced a pronounced increase in cell death processes accompanied by a decrease in survival processes compared to the cells treated with cisplatin or TNF-α alone, and that cisplatin inhibited the typical TNF-α-induced pathways.

3.3. Cisplatin/TNF-α treatment leads to increased gene expression of kidney injury markers and specific cytokines and chemokines

Over the past years, several new kidney injury markers have been identified including kidney injury molecule 1 (KIM-1) and lipocalin 2 (NGAL) (21). To determine whether combined cisplatin/TNF-α treatment enhanced the gene expression of such markers compared to cisplatin treatment alone, we analyzed the expression of genes related to kidney injury as identified by IPA. The expression of these genes was either increased or decreased in cisplatin/TNF-α treated cells compared to cisplatin or TNF-α treated cells correlating with the gene expression pattern of these markers during kidney injury (Fig. 3A). The up-regulated markers included brain natriuretic peptide (BNP), NGAL and KIM-1 (Fig. 3A, up-regulated). These markers are promising kidney injury markers currently evaluated (21). Other up-regulated genes are genes involved in AKI but not yet regarded as potential markers, such as the bradykinin receptor B2 (BDKRB2), the heparin-binding EGF-like growth factor (HBEGF), the cyclic AMP-dependent transcription factor ATF-3, cathepsin L (CTSL), the urokinase receptor (uPAR) and the receptor for advanced glycation endproducts (RAGE) (22-28). Other markers are involved in oxidative stress or inflammation, such as hemeoxygenase 1 (HO-1), cyclooxygenase-2 (COX-2), Granulocyte colony-stimulating factor (GCSF) and interleukin 6 (IL-6) (29-31). However, it is important to note that the gene expression of some markers, such as KIM-1, were already up-regulated by TNF-α treatment alone. The down-regulated markers included the mineralocorticoid receptor (MR), the vitamin D receptor (vdr), megalin (Lrp2) as well as others (Fig. 3A, down-regulated). These markers

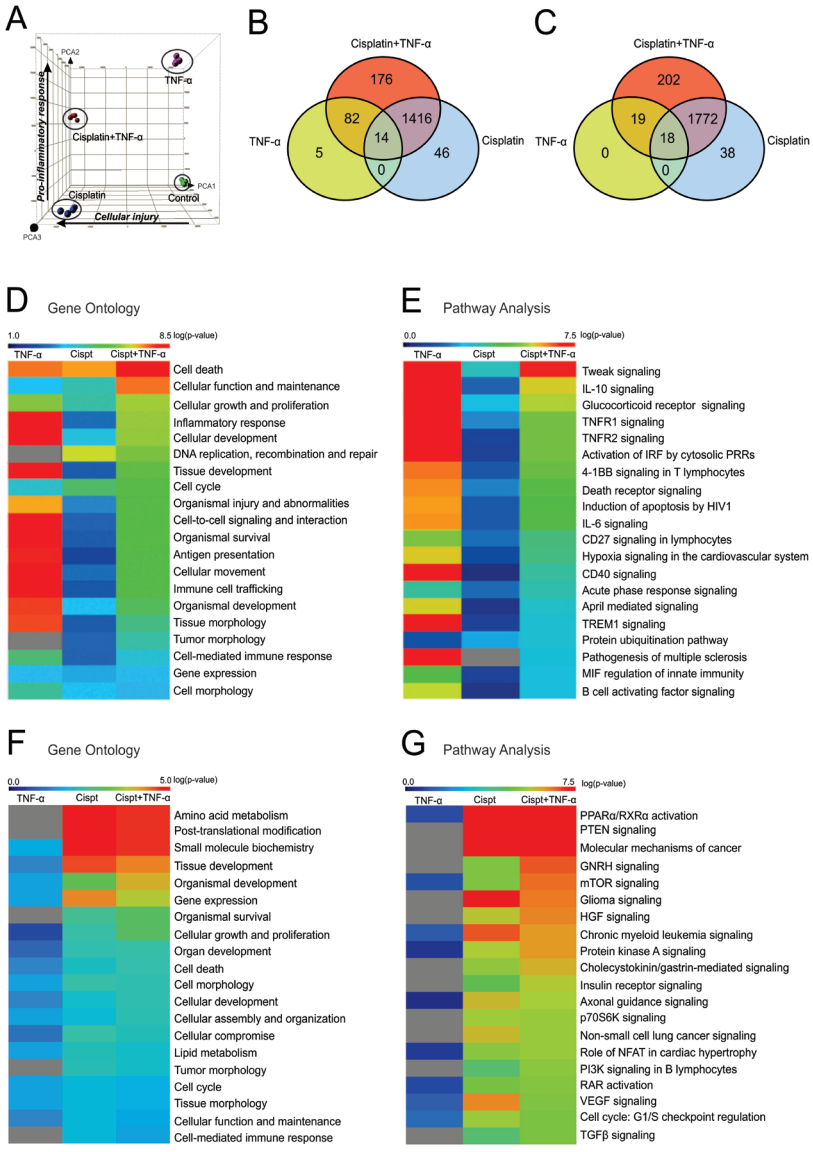

Figure 2. Cisplatin/TNF-α treatment enhances cell death, reduces survival pathways and cisplatin decreases the TNFa-induced inflammatory pathways. IM-PTECs were pre-exposed to TNF-α (8 ng/ml) for 30 min followed by cisplatin 5 μM treatment for 8 h. Following hybridization and RMA normalization, the total gene set was analyzed with a PCA analysis with the Spotfire software. The labels of cellular injury and pro-inflammatory response (in bold and italic) were overlaid from apoptosis measurements and gene expression data (A). The genes with ≥ 2.0-fold-change and FDR ≤ 0.01 were further selected. The uniquely differentially expressed genes with the combined cisplatin/TNF-α treatment were then separated into up-regulated genes (B, D and E) and down-regulated genes (C, F and G). A Venn diagram was made for the up-regulated genes (B) and down-regulated genes (C). Using the IPA software, a gene ontology (D and F) and pathways analysis (E and G) were performed.

have been shown as well to be related to kidney injury (27, 32, 33). Together these data indicate that the expression levels of the kidney injury markers reflect the increased cell death observed in cisplatin/TNF-α treated IM-PTECs.

Since several cytokines were identified among the genes related to kidney injury, we investigated whether the combined cisplatin/TNF-α treatment stimulated the expression of some specific cytokines and chemokines. Our gene array analysis clearly showed a drastic increase in some inflammatory related genes under cisplatin/TNF-α conditions (Fig. 3B). These genes included macrophage inflammatory protein 2 (MIP2), monocyte chemo-attractant protein 1 (MCP1) and IL-6, which have been shown to be increased in cisplatin-induced nephrotoxicity *in vivo* (14, 31). MIP2 and MCP1 contribute to the kidney injury, while IL-6 seems to have a protective role. In addition, G-CSF and Granulocyte macrophage colony-stimulating factor (GM-CSF) were up-regulated, which have been shown to be released in other kidney injury models *in vivo* (renal ischemia-reperfusion or other diseases) and contributed to immune cell infiltration and associated injury (1, 34). Some cytokine genes were down-regulated compared to TNF-α alone, including the interferon-gamma-inducible protein 9 (IP9), the interferon-gamma-inducible protein 10 (IP10) and Regulated upon Activation, Normal T-cell Expressed, and Secreted protein (RANTES). All together, these data showed that treatment of our IM-PTECs with a combination of cisplatin and TNF-α, but not cisplatin alone, resulted in up-regulation of the gene expression of kidney injury markers and specific inflammatory mediators, thereby mimicking the cisplatin-induced nephrotoxicity response observed *in vivo*. Our *in vitro* model is therefore a good model system to study nephrotoxicant-induced AKI *in vitro*.

3.4. Cisplatin/TNF-α treatment enhances genes transcribed by AP1/c-Jun and reduces genes transcribed by NF-κB

In order to identify which transcription factors likely regulate the differentially expressed genes in our analysis, a transcription factor analysis was performed with Metacore™ using in total the top 1000 up- and down- regulated genes in cisplatin/TNF-α, cisplatin or TNF-α treated cells. This analysis revealed that several transcription factors are implicated in the transcription of the top differentially expressed genes in cisplatin/TNF-α treated IM-PTECs, including the hepatocyte nuclear factor 4 α (HNF4-α), the activator protein 1 (AP1) (including c-Jun), the cAMP responsive element binding protein 1 (CREB1), the estrogen receptor (ESR1α), p53 and NF-κB (including RelA, NF-κB1 and c-Rel) (Fig. 3C). These transcription factors are known to regulate several

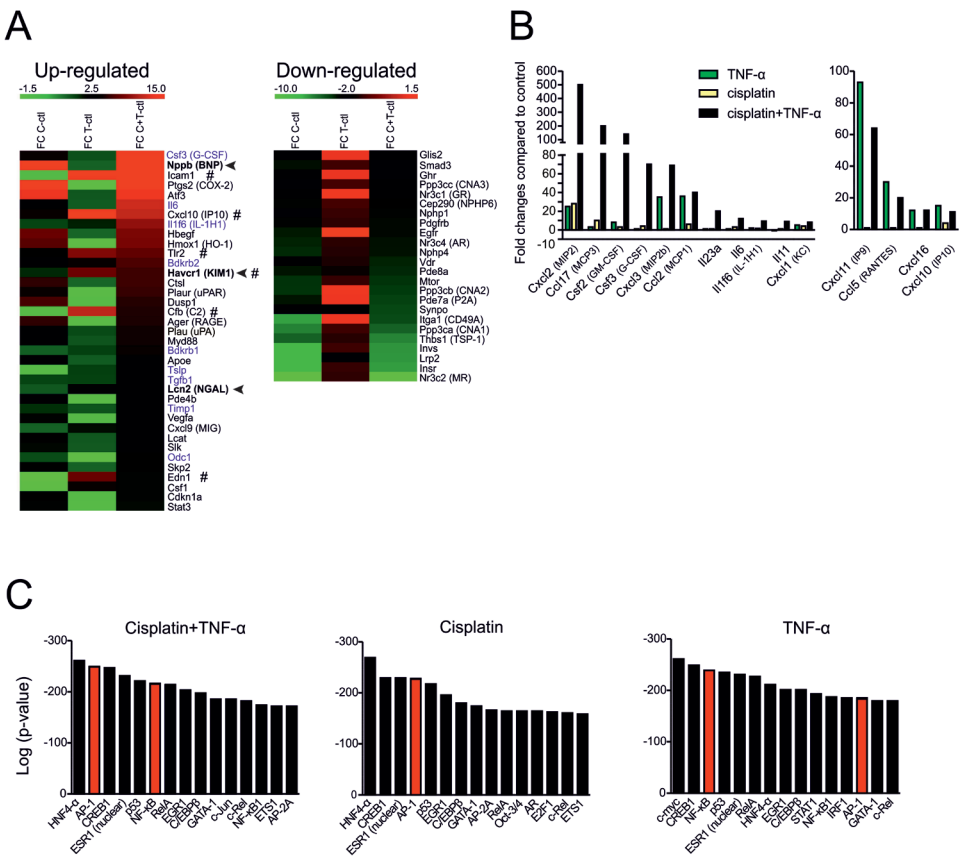

Figure 3. Cisplatin/TNF-α treatment leads to increased gene expression of kidney injury markers and specific cytokines and chemokines. The gene expression values of genes defined by the IPA software as associated with kidney injury in the cisplatin/TNF-α cells was represented in a heatmap (FC, fold change; C, cisplatin; T, TNF-α; C + T, cisplatin/TNF-α; and ctl, control). The corresponding protein names, when differing from the gene name, are included in brackets. The kidney injury markers currently evaluated are depicted in bold and marked with an arrow and the markers up-regulated by cisplatin/TNF-α co-treatment only are depicted in blue. The markers changing already with cisplatin and TNF-α treatment only are marked by a pound sign (A). Gene expression values of cytokines and chemokines were compared between the different treatments and are represented as fold changes compared to control. The corresponding protein names, when differing from the gene name, are included in brackets (B). A transcription factor analysis was performed with the Metacore software for the 1000 top differentially regulated genes for each treatment. The 15 most significant transcription factors (P-value <0.001) are depicted with their log(P-value) for each condition (C).

cellular processes such as cellular proliferation and differentiation (HNF4-α, CREB1), the DNA damage response (p53, ESR1), apoptosis (p53, AP1, NF-κB, CREB1) as well as inflammation (AP-1, NF-κB, CREB1) (35-39). It is also important to note that most of

these transcription factors have been shown to interact with NF-κB to cooperatively regulate some specific genes (40). In the cisplatin treated cells, the main transcription factors were HNF4-α, CREB1, ESR1α, AP1 and p53 and NF-κB was involved in a much lesser extent. In the TNF-α treated cells, the myelocytomatosis oncogene (c-myc), CREB1, NF-κB (including RelA, NF-κB1 and c-Rel) and p53 were part of the main transcription factors involved. This analysis reveals that cisplatin/TNF-α treatment reduced the number of genes transcribed by NF-κB compared to TNF-α treatment and enhanced the number of genes transcribed by AP1/c-Jun compared to cisplatin and TNF-α treatment.

3.5. Cisplatin/TNF-α co-treatment enhances JNK-induced cell killing

AP-1, identified by Metacore™ as a major factor involved in cisplatin/TNF-α treated cells, is a transcription factor composed of several members including the transcription factor c-Jun (41) and is involved in the transcription of inflammatory genes as well as in the regulation of apoptosis (36, 41). c-Jun is activated through JNK-mediated phosphorylation and JNK was already shown to be activated by cisplatin *in vitro* and *in vivo* (42, 43). Therefore, the activation status of JNK and c-Jun was determined after exposure of the IM-PTECs to TNF-α alone, cisplatin alone or cisplatin and TNF-α. Cisplatin alone caused sustained JNK phosphorylation which was further significantly increased with cisplatin/TNF-α co-exposure (Fig. 4A). The subsequent c-Jun phosphorylation was only enhanced and sustained in cisplatin/TNF-α treated cells (Fig. 4A). No difference was observed between cisplatin alone and cisplatin/TNF-α co-treatment for the other MAPKs, ERK and p38 (data not shown).

In order to define whether cisplatin/TNF-α treatment led to activation and prolongation of JNK via the DNA damage or ER stress response pathway, IM-PTECs were treated with other DNA damaging agents – doxorubicine, etoposide and MMS – and to the ER stress agent tunicamycin. Enhanced and prolonged JNK phosphorylation as well as c-Jun phosphorylation was observed with all DNA damaging agents as well as the ER stress agent tunicamycin, indicating that cisplatin/TNF-α dependent sustained activation of JNK might involve a combination of cellular stresses (Fig. 4C).

It was previously reported that JNK phosphorylation status balances the cells between cell death and survival (12). Therefore, the role of JNK in our IM-PTECS was evaluated by inhibiting JNK by 30 minutes pre-treatment with the JNK inhibitor SP600125 (20 μM) followed by cisplatin/TNF-α exposure. JNK inhibition led to a

reduction of c-Jun phosphorylation (Fig. 4B). Under these conditions cisplatin/TNF-α-induced apoptosis was partially reduced (Fig. 4D). These data indicate that sustained activation of JNK and subsequent c-Jun activation induced by cisplatin/TNF-α co-treatment leads to sensitization of the IM-PTECs.

3.6. Cisplatin decreases TNF-α-induced NF-κB signalling

Since the number of genes transcribed by the transcription factor NF-κB was shown to be reduced by cisplatin/TNF-α treatment compared to TNF-α in our *in vitro* model. Under normal conditions, NF-κB is sequestered in the cytoplasm by its inhibitor IκB. Upon TNF-α exposure, NF-κB is freed from its inhibitor and translocates from the cytoplasm into the nucleus where it can start the transcription of its target genes (44). Therefore, NF-κB nuclear translocation was examined over time by following the localization of one of the main NF-κB subunits, p65 (RelA). Cisplatin co-exposure with TNF-α reduced p65 translocation to the nucleus compared to TNF-α alone (Fig. 5A). This reduced nuclear translocation was accompanied by decreased NF-κB-mediated gene transcription as determined by the activation of a general NF-κB luciferase construct (Fig. 5B). The effect of cisplatin/TNF-α exposure on NF-κB was independent of its inhibitor IκBα, since the phosphorylation of IκBα accompanied by its degradation following TNF-α addition was observed for both TNF-α and cisplatin/TNF-α treatments (Fig. 5C). An increase in phosphorylation of IκBα and its turnover can be observed with cisplatin/TNF-α exposure compared to TNF-α and can be explained by a decrease in tumor necrosis factor alpha-induced protein 3 (TNAFAIP3/A20) levels due to NF-κB transcriptional inhibition.

To determine whether the observed perturbation in the NF-κB pathway was associated with the increased percentage of apoptosis observed under cisplatin/TNF-α condition (Fig. 1), NF-κB activation was inhibited by pre-treatment with the IKKα/β inhibitor wedelolactone (20 μM) for 30 minutes before cisplatin/TNF-α treatment. Wedelolactone decreased TNF-α-induced NF-κB transcription (Fig. 5D), which was accompanied by a sensitization of the IM-PTECs for cisplatin/TNF-α-induced apoptosis (Fig. 5E). Furthermore, lentiviral shRNA-based stable knockdown of p65, as determined by Western blot, also sensitized the IM-PTECs to cisplatin/TNF-α-induced apoptosis (Fig. 5F). These data demonstrate that inhibition of NF-κB signalling under cisplatin/TNF-α conditions is associated with the observed enhancement in IM-PTEC apoptotic cell death.

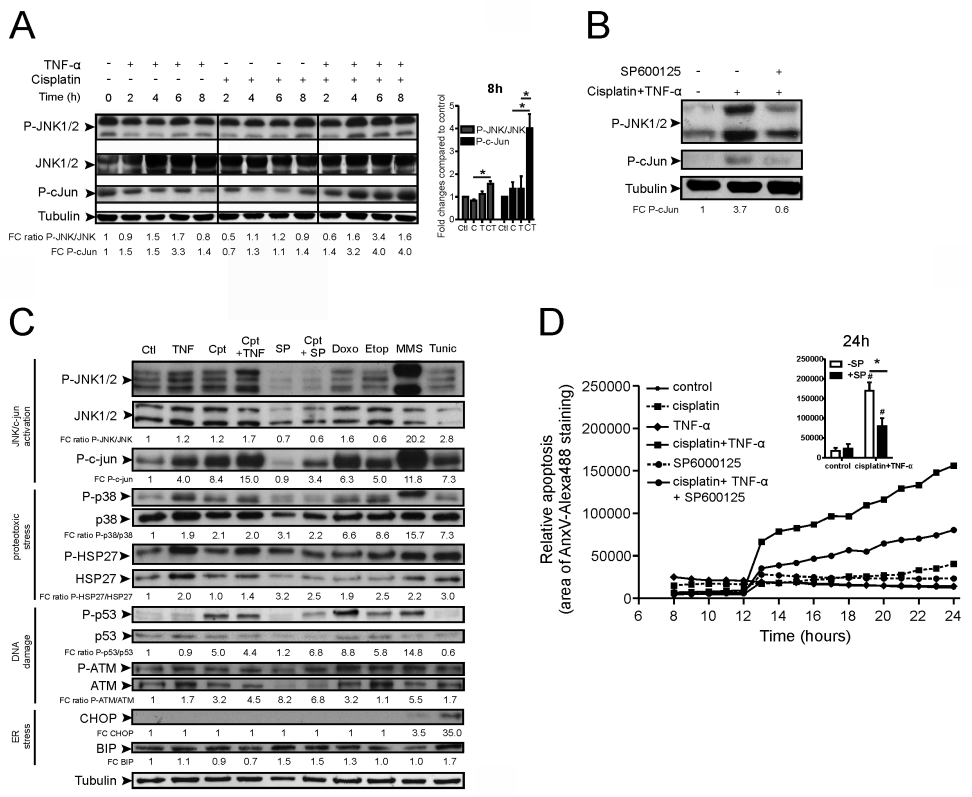

Figure 4. Cisplatin/TNF-α co-treatment enhances JNK-induced cell killing. IM-PTECs were pre-exposed to TNF-α (8 ng/ml) for 30 min followed by cisplatin 10 μM treatment. JNK and c-Jun activation was assessed over time by Western blot analysis (A–C). Quantification and statistics are represented for the 8 h timepoint (ctl, control; C, cisplatin; T, TNF-α; CT, cisplatin + TNF-α) (A). JNK activation was inhibited by pre-exposure of the IM-PTECS to the JNK-specific inhibitor SP600125 (20 mM) for 30 min prior to cisplatin/TNF-α exposure (B–D). The effective JNK inhibition was assessed by Western blot analysis after 8 h of exposure to cisplatin (B). IM-PTECs were exposed to cisplatin 10 μM and several other DNA damaging agents – doxorubicine (3 μM), etoposide (5 μM), MMS (50 μg/ml) – and to the ER stress agent tunicamycin (10 μg/ml) for 8 h and the phosphorylation of several proteins implicated in different cellular stresses was assessed (ctl, control; TNF, TNF-α; Cpt, cisplatin; Cpt + TNF, cisplatin + TNF-α; SP, SP600125; Cpt + SP, cisplatin + SP600125; Doxo, doxorubicine; Etop, etoposide; Tunic, tunicamycin) (C). Tubulin was used as loading control and the quantification indicated is the mean of three independent experiments for all Western analysis (A–C). Apoptosis was followed over time after exposure using Annexin V-Alexa488 staining and automated imaging on a BD pathway 855 imager (SP, SP600125) (D). Data are the mean of three independent experiments. *P ≤ 0.05 and #P ≤ 0.05 compared to vehicle-treated cells.

3.7. Initial inhibition of NF-κB signalling causes sustained JNK activation, resulting in prolonged NF-κB inhibition; a cisplatin/TNF-α feedback mechanism

It has previously been shown that inhibition of NF-κB results in sustained JNK activation (45-47). Yet, sustained JNK activation may also inhibit NF-κB activation and shift cells towards a pro-apoptotic program (20,48,49). Since cisplatin/TNF-α treatment of IM-PTECs resulted in reduced NF-κB signalling and sustained JNK activation, the role of NF-κB in JNK activation and vice versa was investigated.

To determine whether cisplatin/TNF-α mediated NF-κB inhibition at early time-points (e.g. before 2 hours) was dependent on JNK activation, c-Jun phosphorylation levels were determined at 15-120 minutes after exposure. The levels of JNK and c-Jun phosphorylation were not increased at early time-points, prior to NF-κB inactivation, indicating that the initial inhibition of NF-κB was independent of JNK (Fig. 6A). To verify whether the observed inhibition of NF-κB could result in sustained JNK activation, the activation status of JNK and c-Jun was determined after NF-κB inhibition in combination with cisplatin/TNF-α treatment. The phosphorylation of c-Jun significantly increased when NF-κB was inhibited by either the IKKα/β inhibitor wedelolactone (20 μM) or by stable knockdown of p65 in combination with cisplatin/TNF-α treatment (Fig. 6B). These data suggest that an initial inhibition of NF-κB activation may result in sustained JNK activation.

Next we determined whether JNK is involved in further inhibition of NF-κB activity. While treatment with the JNK inhibitor SP600125 alone or in combination with cisplatin slightly induced p65 nuclear translocation after 60 minutes of exposure (data not shown), pre-treatment with the JNK inhibitor followed by cisplatin/TNF-α exposure induced a significant increase in p65 nuclear translocation (Fig. 6C). The inhibitor alone and with cisplatin (in a lesser extent) already induced p65 translocation at later time points but at a much lesser extent than in combination with cisplatin/TNF-α treatment (data not shown). Furthermore, this increase in p65 nuclear translocation at 1 hour was associated with increased NF-κB transcriptional activity at 4 hours (Fig. 6D).

Together our data suggest that the synergistic effect of cisplatin and TNF-α on apoptosis of renal proximal tubular cells involves a feedback mechanism in which cisplatin inhibits TNF-α-induced NF-κB signalling resulting in sustained JNK activation, which subsequently further reduces NF-κB signalling, thereby enhancing cell death.

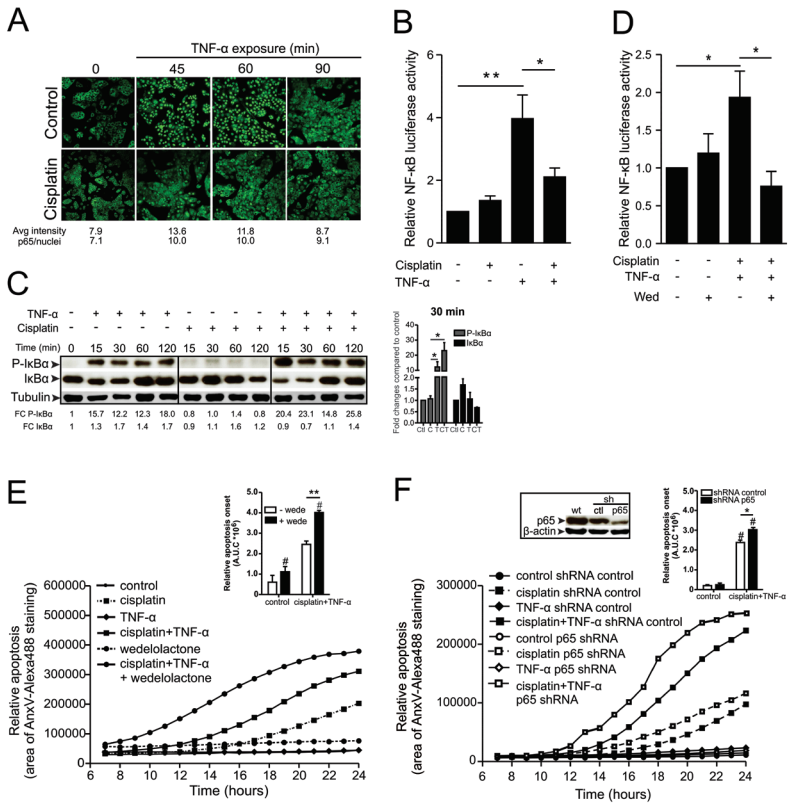

Figure 5. Cisplatin reduces TNF-α-induced NF-κB signalling. IM-PTECs were pre-exposed to TNF-α (8 ng/ml) for 30 min followed by cisplatin 10 μM treatment. The effect of cisplatin/TNF-α exposure on p65 translocation into the nucleus was investigated over time by immunofluorescence staining of p65 (green). The cells were imaged using a Nikon TiE2000 confocal microscope. p65 translocation was quantified by determining the average intensity of p65/nuclei. (A). NF-κB transcriptional activity was investigated using a NF-κB luciferase reporter construct. The luciferase activity was measured after 4 h exposure. Results are expressed as ratios of the luciferase activity in non-exposed cells over exposed cells and represent the means from five independent experiments (B and D). Total and phosphorylated IκBα levels were followed over time by Western blot analysis. The quantification indicated is the mean of three independent experiments. Quantification and statistics are represented for the 30 min timepoint (ctl, control; C, cisplatin; T, TNF-α; CT, cisplatin + TNF-α) (C). NF-κB activity was inhibited by pre-exposure of the IM-PTECs to the IKKα/β inhibitor wedelolactone (20 μM) for 30 min prior to cisplatin/TNF-α exposure (D and E). The effective NF-κB inhibition was assessed by luciferase activity measurement (wed, wedelolactone) (D). In addition, stable p65 knock-down cells were generated using lentiviral shRNA vectors. Apoptosis of IM-PTECs after wedelolactone pre-treatment or in IM-PTECs with p65 knock-down was followed over time after cisplatin exposure in the presence/absence of TNF-α using Annexin V-Alexa488 staining and automated imaging on a BD pathway 855 imager. The relative apoptosis onset represented by the area under the curve (AUC) is depicted for both wedelolactone treatment and p65 knock-down cells (E and F). Quantification of p65 levels in Wt, shControl, and shp65 IM-PTEC cells was done by Western blot analysis. β-actin was used as a loading control (F). Data are the mean of at least three independent experiments SEM. *P ≤ 0.05, ** P ≤ 0.01 and #P ≤ 0.05 compared to vehicle-treated cells.

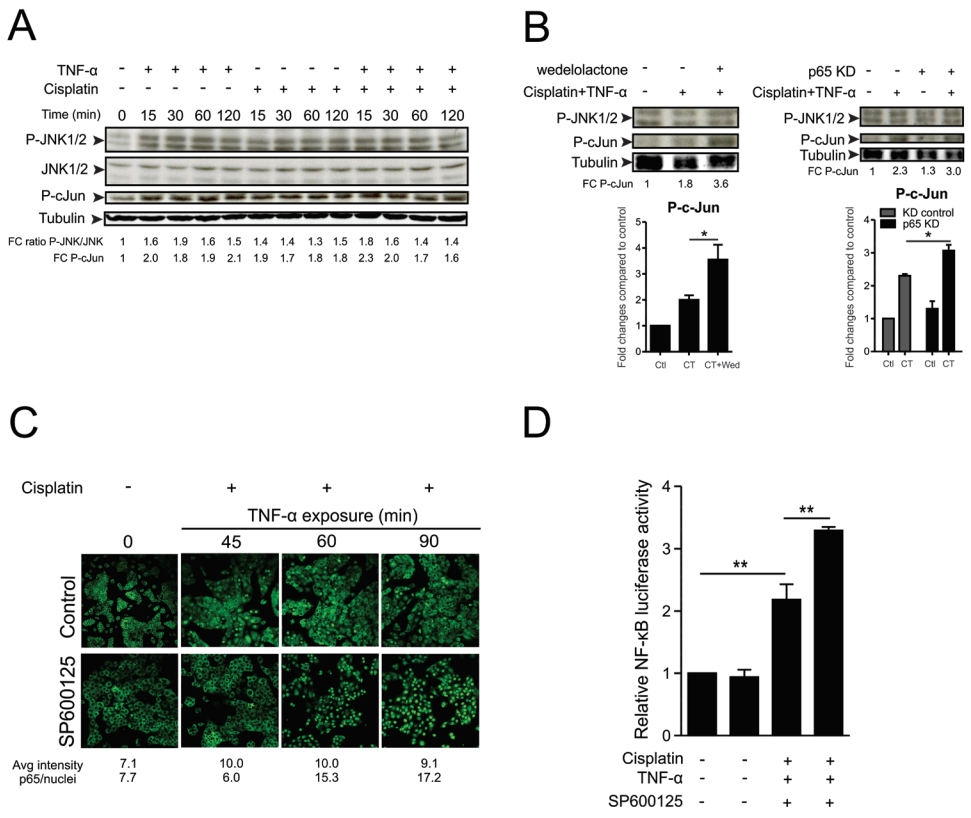

Figure 6. Cisplatin initial inhibition of TNF-α-induced NF-κB signalling is further enhanced by JNK. IM-PTECs were pre-exposed to TNF-α (8 ng/ml) for 30 min followed by cisplatin 10 μM treatment. JNK activation was inhibited by pre-exposure of the IM-PTECS to the JNK-specific inhibitor SP600125 (20 μM) for 30 min prior to cisplatin/TNF-α exposure (A and B). The effect of cisplatin/TNF-α exposure with JNK inhibitor on p65 translocation into the nucleus was investigated over time by immunofluorescence staining of p65 (green). The cells were imaged using a Nikon TiE2000 confocal microscope. p65 translocation was quantified by determining the average intensity of p65/ nuclei. (A). NF-κB transcriptional activity after JNK inhibition was investigated using a NF-κB luciferase reporter construct. The luciferase activity was measured after 4 h of exposure. Results are expressed as ratios of the luciferase activity in non-exposed cells over exposed cells and represent the means from five independent experiments (B). JNK and c-Jun activation was assessed over a short period of time by Western blot analysis (C). The effect of NF-κB inhibition on JNK and c-Jun activation, either by the IKKα/β inhibitor wedelolactone (20 μM) or by p65 knock-down, was assessed by Western blot analysis after 8 h of cisplatin exposure. Quantification and statistics are represented (ctl, control; C, cisplatin; T, TNF-α; CT, cisplatin + TNF-α) (D). Tubulin was used as loading control and the quantification indicated is the mean of three independent experiments for all Western analysis (C and D). Data are the mean of at least three independent experiments SEM. *P ≤ 0.05, **P ≤ 0.01.

3.8. The NF-κB-JNK feedback mechanism leads to a decrease in anti-apoptotic genes and an increase in pro-apoptotic genes

Next, we investigated whether inhibition of NF-κB and activation of JNK by cisplatin/TNF-α treatment is associated with the differential transcription of genes controlling apoptosis. A 2-fold decrease in the transcription of the NF-κB-transcribed anti-apoptotic genes c-IAP2, Bcl2, Bcl-XL and Bruce was observed with the combined cisplatin/TNF-α treatment compared to TNF-α alone (Fig. 7A). This decrease was not changing when the cells were pre-treated with the JNK inhibitor SP600125 (20 μM), indicating that the early inhibition of NF-κB (Fig. 5) may be responsible for the reduced expression of this set of anti-apoptotic genes (Fig.7B). Cisplatin/TNF-α co-treatment also increased the gene expression levels of the two pro-apoptotic genes Bcl2-like kin (Bfk) – a new Bcl2 member involved in DNA damage (50) - and X-linked inhibitor of apoptosis protein associated factor 1 (Xaf1) – an antagonist of XIAP (51) (Fig. 7C). Pre-treatment of the cells with the JNK inhibitor SP600125 (20 μM) significantly decreased the level of Xaf1, but not Bfk to control level, indicating that JNK controlled the transcription of the pro-apoptotic gene Xaf1 (Fig. 7D).

These data indicate that the NF-κB/JNK/c-Jun imbalance leads to a reduction in anti-apoptotic genes accompanied by an increase in pro-apoptotic genes, thereby driving the cells towards enhanced apoptosis (Fig. 7E).

4. Discussion

The clinical application of cisplatin is limited due to its renal toxicity. Cisplatin is known to induce toxicity via activation of various signalling pathways leading to direct tubular cell injury, but is also known to trigger an inflammatory response. TNF-α appears to be a key upstream regulator of this inflammatory response. Although TNF-α is known to play a major role in cisplatin-induced renal toxicity and inflammation, it is not yet clear which pathways synergistically activated by cisplatin and TNF-α lead to an enhancement of renal injury. Our data demonstrate that in renal proximal tubular epithelial cells, TNF-α enhanced cisplatin-induced cell death *in vitro*. This enhancement was associated with an increase in the activation of cell death accompanied by a decrease in survival pathways. Furthermore, the gene expression levels of kidney injury markers were enhanced in cisplatin/TNF-α treated cells accompanied by a dramatic induction of specific cytokines and chemokines gene expression levels mimicking the cisplatin-induced nephrotoxicity response observed *in vivo*. Some kidney injury markers

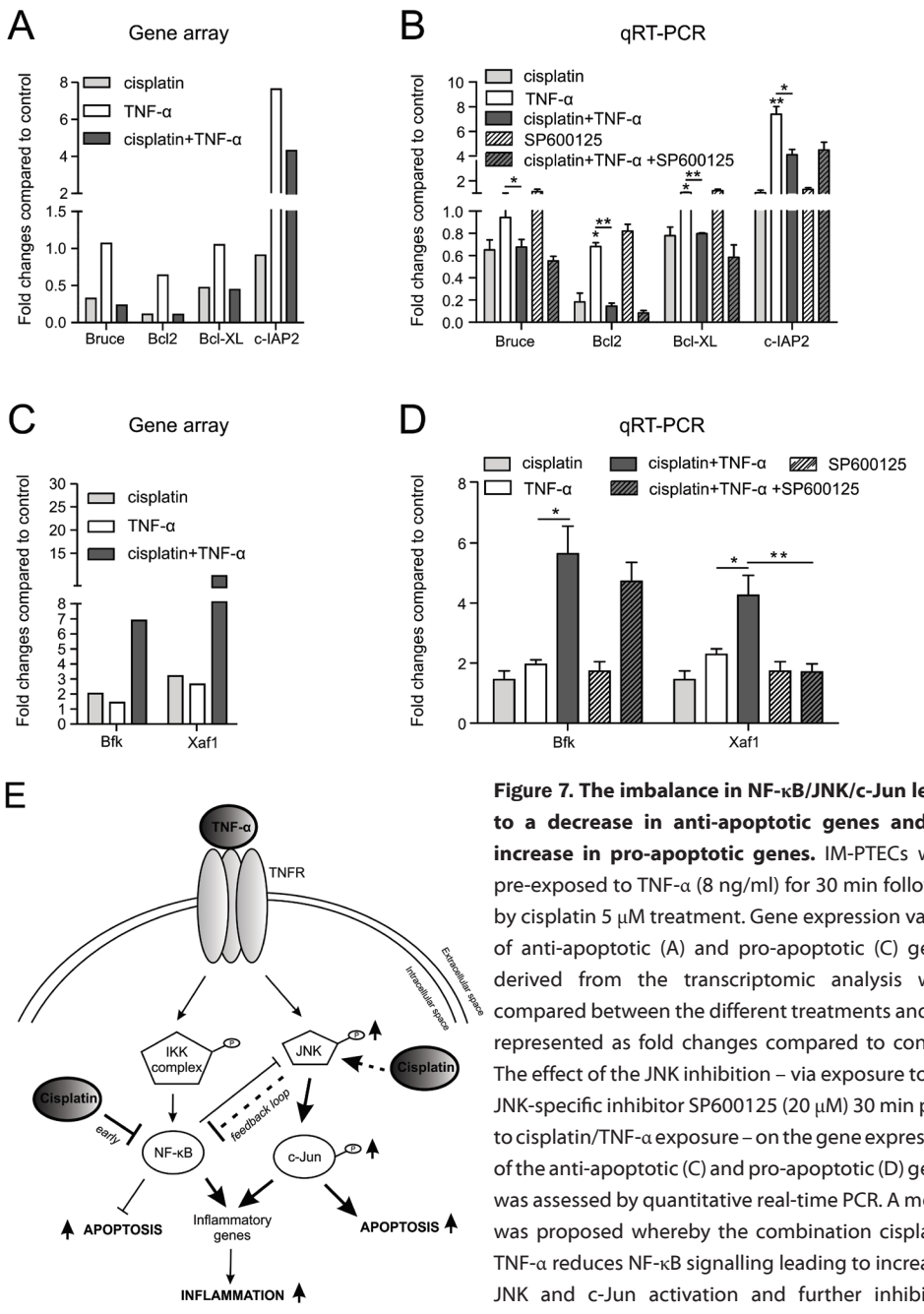

Figure 7. The imbalance in NF-κB/JNK/c-Jun leads to a decrease in anti-apoptotic genes and an increase in pro-apoptotic genes. IM-PTECs were pre-exposed to TNF-α (8 ng/ml) for 30 min followed by cisplatin 5 μM treatment. Gene expression values of anti-apoptotic (A) and pro-apoptotic (C) genes derived from the transcriptomic analysis were compared between the different treatments and are represented as fold changes compared to control. The effect of the JNK inhibition – via exposure to the JNK-specific inhibitor SP600125 (20 μM) 30 min prior to cisplatin/TNF-α exposure – on the gene expression of the anti-apoptotic (C) and pro-apoptotic (D) genes was assessed by quantitative real-time PCR. A model was proposed whereby the combination cisplatin/TNF-α reduces NF-κB signalling leading to increased JNK and c-Jun activation and further inhibiting NF-κB by JNK via a feedback-loop mechanism. The JNK/c-Jun/NF-κB imbalance then affects the transcriptional activation of anti- and pro-apoptotic proteins and of inflammatory genes. Dotted arrows indicate that the effect of cisplatin on JNK activation or JNK inhibition on NF-κB is not indirect (E).

however, such as thrombospondin 1 (TSP-1), were down-regulated with cisplatin/TNF-α treatment. TSP-1 has been shown to be up-regulated during renal I/R injury (52) and diabetic nephropathy (53) and in several cancer cells after cisplatin treatment (54, 55). However, so far no studies showed the role of TSP-1 in cisplatin treated renal cells. In addition to this increase in kidney injury markers and inflammatory mediators, our mechanistic study in this model showed that TNF-α enhanced cisplatin-induced cell death of proximal tubular cells via interfering with NF-κB and JNK activation status. By altering the tightly regulated balance between these pro- and anti-apoptotic proteins, the gene transcription in these cells is shifted towards enhanced injury, cell death and inflammation. These data fit with the model whereby the harmed proximal tubular cells release TNF-α and thereby aggravate the primary renal injury *in vivo*.

Cisplatin/TNF-α treatment affected the NF-κB/JNK/c-Jun balance in three ways. First, cisplatin/TNF-α perturbed the NF-κB signalling by reducing significantly p65 translocation and NF-κB-mediated gene transcription compared to TNF-α treatment. Second, NF-κB inhibition led to enhanced and prolonged JNK phosphorylation and JNK inhibition with the SP600125 inhibitor led to a decrease in cell death. Third, JNK enhanced activation led to further inhibition of the NF-κB signalling pathway and shifted the transcription of genes controlling apoptosis. NF-κB signalling was shown to be essential in IM-PTECs since inhibition of NF-κB activation by the IKKα/β inhibitor wedelolactone or by p65 knock-down sensitized the cells towards cisplatin/TNF-α toxicity. The inhibition of NF-κB signalling affected the transcription of anti-apoptotic genes typically induced by TNF-α in normal cells (such as c-IAP2). TNF-α alone did not cause apoptosis when NF-κB signalling was inhibited by wedelolactone, indicating that TNF-α signalling itself is not the main contributor to the onset of apoptosis but the synergy between TNF-α and the toxic properties of cisplatin is. Our data reveal that the initial inhibition of NF-κB is done by cisplatin and that NF-κB inhibition leads to sustained JNK activation corroborating with previous studies (20, 48, 49). It is known that JNK is activated by ROS and the crosstalk between JNK and NF-κB involves ROS formation (46). It was shown that early/transient JNK activation is dependent upon TRAF, whereas prolonged JNK activation is ROS-dependent (56). However, in our proximal tubular cells, there was no difference in ROS production between cisplatin and cisplatin/TNF-α treatments. Therefore the increase in JNK activation due to NF-κB inhibition in cisplatin/TNF-α treated cells does not seem to be due to increased ROS formation. The inhibition of NF-κB by cisplatin was an IκBα-independent mechanism since P-IκBα induction followed by IκBα degradation was observed in cisplatin/TNF-α treated cells. The compound dehydroxymethylepoxyquinomicin (DHMEQ) was shown

to inhibit NF-κB signalling by inhibiting its translocation to the nucleus without interfering with the activation and degradation of IκBα in Jurkat and COS-1 cells (57). In order to translocate into the nucleus, proteins need to contain a nuclear localization signal (NLS) (58). By checking the nuclear transport of other NLS-containing proteins, Ariga et al. ruled out the impairment of the general transport mechanism and suggested that the compound might bind to p65 or p50. Therefore, it could be that cisplatin (in) directly causes phosphorylation of p65 or binds to it, masking the NLS and preventing it to enter the nucleus.

Furthermore, sustained JNK activation was also responsible for further NF-κB inhibition since JNK inhibition by the inhibitor SP600125 restored p65 translocation and NF-κB-mediated gene transcription. This feedback loop mechanism was already observed in a previous study where RhoA-mediated AP-1 activity promoted expression of cyclooxygenase-2 (COX-2) with consequent feedback inhibition of NF-κB activation through IKKβ (20). This could be a possible explanation for the feedback loop observed in our IM-PTECs.

Moreover, as a consequence of increased JNK phosphorylation, c-Jun phosphorylation was increased. Consequently, the activity of the transcription factor AP-1 was increased with the combined treatment and led to the increased transcription of the pro-apoptotic gene Xaf-1. Bfk, the other pro-apoptotic gene increased with the combined treatment was not dependent upon AP-1 and was most likely activated by DNA damage.

In addition, c-Jun and NF-κB were identified as part of the main transcription factors involved in the regulation of the differentially regulated genes in cisplatin/TNF-α treated cells. c-Jun and NF-κB are known to induce the transcription of several inflammatory proteins and it was already shown that NF-κB and c-Jun cooperatively activated IL-6 in human multiple myeloma cells (59). We propose that the change in the NF-κB/JNK/c-Jun balance brings the cells to transcribe specific inflammatory genes with a well-orchestrated cooperation between c-Jun and NF-κB. Since p65 translocation and in general NF-κB-mediated gene transcription were reduced with cisplatin/TNF-α treatment, we believe that the remaining NF-κB signalling activated is regulating the transcription of the inflammatory genes. NF-κB contains five members: NF-κB1 (p50), NF-κB2 (p52), RelA (p65), RelB and c-Rel that form homo- and heterodimers (44). Therefore, even if p65 translocation was reduced, other NF-κB members could transcribe the inflammatory genes. However, it is not well known which NF-κB dimer combination regulates which gene, especially in the kidney. More in depth study should be done to evaluate which NF-κB member could be involved in the transcription of inflammatory

genes in our IM-PTECs.

In summary, we show that TNF-α enhanced cisplatin-induced renal proximal tubular injury. We propose a mechanism by which the combination cisplatin/TNF-α reduces NF-κB signalling leading to sustained JNK and c-Jun activation. The sustained JNK activation further inhibits NF-κB via a feedback mechanism, thereby affecting the transcriptional activation of anti- and pro-apoptotic molecules and enhancing the transcription of inflammatory genes. These results prove that studying the interaction of nephrotoxic drugs and pro-inflammatory cytokines in an *in vitro* model can be used to give mechanistic insight on drug-induced nephrotoxicity.

Acknowledgements

This work was performed as part of the Netherlands Toxicogenomics Center (NTC)/ Netherlands Genomics Initiative supported by the Dutch Organization for Scientific Research (NWO) grant nr. 050-06-510 and the Dutch Top Institute Pharma project grant D3-201.

References

1. Cohen SM, Lippard SJ. Cisplatin: from DNA damage to cancer chemotherapy. Progress in nucleic acid research and molecular biology 2001;67:93-130.

2. Arany I, Safirstein RL. Cisplatin nephrotoxicity. Semin Nephrol 2003;23:460-464.

3. Pabla N, Dong Z. Cisplatin nephrotoxicity: mechanisms and renoprotective strategies. Kidney international 2008;73:994-1007.

4. Yao X, Panichpisal K, Kurtzman N, Nugent K. Cisplatin nephrotoxicity: a review. The American journal of the medical sciences 2007;334:115-124.

5. Zhang B, Ramesh G, Norbury CC, Reeves WB. Cisplatin-induced nephrotoxicity is mediated by tumor necrosis factor-alpha produced by renal parenchymal cells. Kidney international 2007;72:37-44.

6. Ramesh G, Brian Reeves W. Cisplatin increases TNF-alpha mRNA stability in kidney proximal tubule cells. Renal failure 2006;28:583-592.

7. Ramesh G, Kimball SR, Jefferson LS, Reeves WB. Endotoxin and cisplatin synergistically stimulate TNF-alpha production by renal epithelial cells. American journal of physiology. Renal physiology 2007;292:F812-819.

8. Liu M, Chien CC, Burne-Taney M, Molls RR, Racusen LC, Colvin RB, Rabb H. A pathophysiologic role for T lymphocytes in murine acute cisplatin nephrotoxicity. Journal of the American Society of Nephrology : JASN 2006;17:765-774.

9. Hoffmann A, Baltimore D. Circuitry of nuclear factor kappaB signalling. Immunol Rev 2006;210:171-186.

10. Micheau O, Tschopp J. Induction of TNF receptor I-mediated apoptosis via two sequential

signalling complexes. Cell 2003;114:181-190.

11. Deng Y, Ren X, Yang L, Lin Y, Wu X. A JNK-dependent pathway is required for TNFalpha-induced apoptosis. Cell 2003;115:61-70.

12. Wullaert A, Heyninck K, Beyaert R. Mechanisms of crosstalk between TNF-induced NF-kappaB and JNK activation in hepatocytes. Biochemical pharmacology 2006;72:1090-1101.

13. Fredriksson L, Herpers B, Benedetti G, Matadin Q, Puigvert JC, de Bont H, Dragovic S, et al. Diclofenac inhibits tumor necrosis factor-alpha-induced nuclear factor-kappaB activation causing synergistic hepatocyte apoptosis. Hepatology 2011;53:2027-2041.

14. Ramesh G, Reeves WB. TNF-alpha mediates chemokine and cytokine expression and renal injury in cisplatin nephrotoxicity. The Journal of clinical investigation 2002;110:835-842.

15. Puigvert JC, de Bont H, van de Water B, Danen EH. High-throughput live cell imaging of apoptosis. Curr Protoc Cell Biol 2010;Chapter 18:Unit 18 10 11-13.

16. Stokman G, Qin Y, Genieser HG, Schwede F, de Heer E, Bos JL, Bajema IM, et al. Epac-Rap signalling reduces cellular stress and ischemia-induced kidney failure. Journal of the American Society of Nephrology : JASN 2011;22:859-872.

17. de Graauw M, Tijdens I, Cramer R, Corless S, Timms JF, van de Water B. Heat shock protein 27 is the major differentially phosphorylated protein involved in renal epithelial cellular stress response and controls focal adhesion organization and apoptosis. The Journal of biological chemistry 2005;280:29885-29898.

18. Benjamini YaH, Y. Controlling the False Discovery Rate: A Practical and Powerful Approach to Multiple Testing. Journal of the Royal Statistical Society. Series B (Methodological) 1995;57:289-300.

19. Kelsen DP, Alcock N, Young CW. Cisplatin nephrotoxicity. Correlation with plasma platinum concentrations. Am J Clin Oncol 1985;8:77-80.

20. Brouwers EE, Huitema AD, Beijnen JH, Schellens JH. Long-term platinum retention after treatment with cisplatin and oxaliplatin. BMC Clin Pharmacol 2008;8:7.

21. Bonventre JV, Vaidya VS, Schmouder R, Feig P, Dieterle F. Next-generation biomarkers for detecting kidney toxicity. Nat Biotechnol 2010;28:436-440.

22. Wang PH, Cenedeze MA, Pesquero JB, Pacheco-Silva A, Camara NO. Influence of bradykinin B1 and B2 receptors in the immune response triggered by renal ischemia-reperfusion injury. International immunopharmacology 2006;6:1960-1965.

23. Mulder GM, Nijboer WN, Seelen MA, Sandovici M, Bos EM, Melenhorst WB, Trzpis M, et al. Heparin binding epidermal growth factor in renal ischaemia/reperfusion injury. The Journal of pathology 2010;221:183-192.

24. Cheng CF, Lin H. Acute kidney injury and the potential for ATF3-regulated epigenetic therapy. Toxicology mechanisms and methods 2011;21:362-366.

25. Bauer Y, Hess P, Qiu C, Klenk A, Renault B, Wanner D, Studer R, et al. Identification of cathepsin L as a potential sex-specific biomarker for renal damage. Hypertension 2011;57:795-801.

26. Gueler F, Rong S, Mengel M, Park JK, Kiyan J, Kirsch T, Dumler I, et al. Renal urokinase-type plasminogen activator (uPA) receptor but not uPA deficiency strongly attenuates ischemia reperfusion injury and acute kidney allograft rejection. Journal of immunology 2008;181:1179-1189.

27. Nakamura T, Sato E, Fujiwara N, Kawagoe Y, Koide H, Ueda Y, Takeuchi M, et al. Calcium channel blocker inhibition of AGE and RAGE axis limits renal injury in nondiabetic patients with stage I or II chronic kidney disease. Clinical cardiology 2011;34:372-377.

28. Eleftheriadis T, Antoniadi G, Liakopoulos V, Antoniadis N, Stefanidis I, Galaktidou G. Vitamin D receptor activators and response to injury in kidney diseases. Journal of nephrology 2010;23:514-524.

29. Duann P, Lianos EA. Mechanisms of HO-1 mediated attenuation of renal immune injury: a gene profiling study. Translational research : the journal of laboratory and clinical medicine

2011;158:249-261.

30. Wei Q, Hill WD, Su Y, Huang S, Dong Z. Heme oxygenase-1 induction contributes to renoprotection by G-CSF during rhabdomyolysis-associated acute kidney injury. American journal of physiology. Renal physiology 2011;301:F162-170.

31. Mitazaki S, Honma S, Suto M, Kato N, Hiraiwa K, Yoshida M, Abe S. Interleukin-6 plays a protective role in development of cisplatin-induced acute renal failure through upregulation of anti-oxidative stress factors. Life sciences 2011;88:1142-1148.

32. Motoyoshi Y, Matsusaka T, Saito A, Pastan I, Willnow TE, Mizutani S, Ichikawa I. Megalin contributes to the early injury of proximal tubule cells during nonselective proteinuria. Kidney international 2008;74:1262-1269.

33. Shibata S, Fujita T. Mineralocorticoid receptors in the pathophysiology of chronic kidney diseases and the metabolic syndrome. Molecular and cellular endocrinology 2011.

34. Timoshanko JR, Kitching AR, Semple TJ, Holdsworth SR, Tipping PG. Granulocyte macrophage colony-stimulating factor expression by both renal parenchymal and immune cells mediates murine crescentic glomerulonephritis. Journal of the American Society of Nephrology : JASN 2005;16:2646-2656.

35. Lucas B, Grigo K, Erdmann S, Lausen J, Klein-Hitpass L, Ryffel GU. HNF4alpha reduces proliferation of kidney cells and affects genes deregulated in renal cell carcinoma. Oncogene 2005;24:6418-6431.

36. Schonthaler HB, Guinea-Viniegra J, Wagner EF. Targeting inflammation by modulating the Jun/AP-1 pathway. Ann Rheum Dis 2011;70 Suppl 1:i109-112.

37. Schultz-Norton JR, Ziegler YS, Nardulli AM. ERalpha-associated protein networks. Trends Endocrinol Metab 2011;22:124-129.

38. Wen AY, Sakamoto KM, Miller LS. The role of the transcription factor CREB in immune function. Journal of immunology 2010;185:6413-6419.

39. May P, May E. Twenty years of p53 research: structural and functional aspects of the p53 protein. Oncogene 1999;18:7621-7636.

40. Perkins ND. Integrating cell-signalling pathways with NF-kappaB and IKK function. Nat Rev Mol Cell Biol 2007;8:49-62.

41. Hess J, Angel P, Schorpp-Kistner M. AP-1 subunits: quarrel and harmony among siblings. Journal of cell science 2004;117:5965-5973.

42. Arany I, Megyesi JK, Kaneto H, Price PM, Safirstein RL. Cisplatin-induced cell death is EGFR/src/ERK signalling dependent in mouse proximal tubule cells. American journal of physiology. Renal physiology 2004;287:F543-549.

43. Francescato HD, Costa RS, Junior FB, Coimbra TM. Effect of JNK inhibition on cisplatin-induced renal damage. Nephrology, dialysis, transplantation : official publication of the European Dialysis and Transplant Association - European Renal Association 2007;22:2138-2148.

44. Hayden MS, Ghosh S. Shared principles in NF-kappaB signalling. Cell 2008;132:344-362.

45. Tang G, Minemoto Y, Dibling B, Purcell NH, Li Z, Karin M, Lin A. Inhibition of JNK activation through NF-kappaB target genes. Nature 2001;414:313-317.

46. Bubici C, Papa S, Pham CG, Zazzeroni F, Franzoso G. NF-kappaB and JNK: an intricate affair. Cell cycle 2004;3:1524-1529.

47. De Smaele E, Zazzeroni F, Papa S, Nguyen DU, Jin R, Jones J, Cong R, et al. Induction of gadd45beta by NF-kappaB downregulates pro-apoptotic JNK signalling. Nature 2001;414:308-313.

48. Kesanakurti D, Chetty C, Bhoopathi P, Lakka SS, Gorantla B, Tsung AJ, Rao JS. Suppression of MMP-2 attenuates TNF-alpha induced NF-kappaB activation and leads to JNK mediated cell death in glioma. PLoS One 2011;6:e19341.

49. Lee YH, Schiemann WP. Fibromodulin suppresses nuclear factor-kappaB activity by inducing

the delayed degradation of IKBA via a JNK-dependent pathway coupled to fibroblast apoptosis. The Journal of biological chemistry 2011;286:6414-6422.

50. Kruidering M, van de Water B, Zhan Y, Baelde JJ, Heer E, Mulder GJ, Stevens JL, et al. Cisplatin effects on F-actin and matrix proteins precede renal tubular cell detachment and apoptosis in vitro. Cell death and differentiation 1998;5:601-614.

51. Qin Y, Stokman G, Yan K, Ramaiahgari S, Verbeek F, de Graauw M, van de Water B, et al. cAMP signalling protects proximal tubular epithelial cells from cisplatin-induced apoptosis via activation of Epac. British journal of pharmacology 2012;165:1137-1150.

52. Thakar CV, Zahedi K, Revelo MP, Wang Z, Burnham CE, Barone S, Bevans S, et al. Identification of thrombospondin 1 (TSP-1) as a novel mediator of cell injury in kidney ischemia. The Journal of clinical investigation 2005;115:3451-3459.

53. Lu A, Miao M, Schoeb TR, Agarwal A, Murphy-Ullrich JE. Blockade of TSP1-dependent TGF-beta activity reduces renal injury and proteinuria in a murine model of diabetic nephropathy. The American journal of pathology 2011;178:2573-2586.

54. Peng X, Li W, Tan G. Reversal of taxol resistance by cisplatin in nasopharyngeal carcinoma by upregulating thromspondin-1 expression. Anti-cancer drugs 2010;21:381-388.

55. Xu B, Liu P, Li J, Lu H. c-MYC depletion potentiates cisplatin-induced apoptosis in head and neck squamous cell carcinoma: involvement of TSP-1 up-regulation. Annals of oncology : official journal of the European Society for Medical Oncology / ESMO 2010;21:670-672.

56. Nakano H, Nakajima A, Sakon-Komazawa S, Piao JH, Xue X, Okumura K. Reactive oxygen species mediate crosstalk between NF-kappaB and JNK. Cell death and differentiation 2006;13:730-737.

57. Ariga A, Namekawa J, Matsumoto N, Inoue J, Umezawa K. Inhibition of tumor necrosis factor-alpha-induced nuclear translocation and activation of NF-kappaB by dehydroxymethylepoxyquinomicin. The Journal of biological chemistry 2002;277:24625-24630.

58. Pemberton LF, Paschal BM. Mechanisms of receptor-mediated nuclear import and nuclear export. Traffic 2005;6:187-198.

59. Xiao W, Hodge DR, Wang L, Yang X, Zhang X, Farrar WL. NF-kappaB activates IL-6 expression through cooperation with c-Jun and IL6-AP1 site, but is independent of its IL6-NFkappaB regulatory site in autocrine human multiple myeloma cells. Cancer biology & therapy 2004;3:1007-1017.

4